Brief Communication | Experimental and Others

http://dx.doi.org/10.3348/kjr.2015.16.4.791
pISSN 1229-6929 · eISSN 2005-8330
Korean J Radiol 2015;16(4):791-797

Korean Journal of Radiology
KJR

Permeability Parameters Measured with Dynamic Contrast-Enhanced MRI: Correlation with the Extravasation of Evans Blue in a Rat Model of Transient Cerebral Ischemia

Hyun Seok Choi, MD[1], Sung Soo Ahn, MD[2], Na-Young Shin, MD[2], Jinna Kim, MD, PhD[2], Jae Hyung Kim, MD, PhD[3], Jong Eun Lee, PhD[4], Hye Yeon Lee, MD, PhD[4], Ji Hoe Heo, MD, PhD[5], Seung-Koo Lee, MD, PhD[2]

[1]Department of Radiology, College of Medicine, The Catholic University of Korea, Seoul 137-701, Korea; Departments of [2]Radiology, [4]Anatomy, and [5]Neurology, College of Medicine, Yonsei University, Seoul 120-752, Korea; [3]Department of Radiology, College of Medicine, Seoul National University, Seoul 110-744, Korea

Objective: The purpose of this study was to correlate permeability parameters measured with dynamic contrast-enhanced magnetic resonance imaging (DCE-MRI) using a clinical 3-tesla scanner with extravasation of Evans blue in a rat model with transient cerebral ischemia.

Materials and Methods: Sprague-Dawley rats (n = 13) with transient middle cerebral artery occlusion were imaged using a 3-tesla MRI with an 8-channel wrist coil. DCE-MRI was performed 12 hours, 18 hours, and 36 hours after reperfusion. Permeability parameters (K^{trans}, v_e, and v_p) from DCE-MRI were calculated. Evans blue was injected after DCE-MRI and extravasation of Evans blue was correlated as a reference with the integrity of the blood-brain barrier. Correlation analysis was performed between permeability parameters and the extravasation of Evans blue.

Results: All permeability parameters (K^{trans}, v_e, and v_p) showed a linear correlation with extravasation of Evans blue. Among them, K^{trans} showed highest values of both the correlation coefficient and the coefficient of determination (0.687 and 0.473 respectively, $p < 0.001$).

Conclusion: Permeability parameters obtained by DCE-MRI at 3-T are well-correlated with Evans blue extravasation, and K^{trans} shows the strongest correlation among the tested parameters.

Index terms: *Brain ischemia; Animal models; Blood-brain barrier; Dynamic contrast-enhanced MRI; Kinetic modeling*

INTRODUCTION

Ischemic stroke is one of the leading causes of death in elderly patients. Intravenous tissue plasminogen activator present within three hours of the onset of an event has been proven to improve clinical outcome (1). However, thrombolytic agents are associated with symptomatic intracerebral hemorrhage (ICH) (2, 3). Many efforts have been made to identify and predict the hemorrhagic transformation. Among the many independent risk factors of symptomatic ICH, hypodensity on computed tomography has been reported to be an image-based risk factor (3-7). There have also been studies using diffusion- or perfusion-weighted magnetic resonance images (8-14). The studies have showen that the area with decreased perfusion, decreased apparent diffusion coefficient, and later reperfusion is associated with hemorrhagic transformation. Although the studies showed promising results for

Received October 14, 2014; accepted after revision March 16, 2015.

Corresponding author: Seung-Koo Lee, MD, PhD, Department of Radiology, College of Medicine, Yonsei University, 50-1 Yonsei-ro, Seodaemun-gu, Seoul 120-752, Korea.
• Tel: (822) 2228-2373 • Fax: (822) 393-3035
• E-mail: slee@yuhs.ac

predicting hemorrhagic transformation, their observations are not directly targeted to the blood-brain interface. Permeability imaging using dynamic contrast-enhanced MRI (DCE-MRI) can measure the integrity of the blood-brain barrier (BBB) (15-22). Because microvascular permeability plays an important role in the pathologic process of a stroke, disruption of the BBB is not only associated with hemorrhagic transformation but also with the evolution of the stroke (23-25). Small animal models are indispensable for pre-clinical research. However, because institutes with dedicated *in-vivo* animal MR systems and coils are limited, few studies have investigated permeability imaging using an animal model. Therefore, the purpose of this study was to correlate permeability parameters measured with DCE-MRI using a clinical 3-T scanner with extravasation of Evans blue in a rat transient cerebral ischemic model.

MATERIALS AND METHODS

Middle Cerebral Artery Occlusion Model

This animal study was approved by and performed in accordance with the institutional guidelines of the Association for Assessment and Accreditation of Laboratory Animal Care International. Thirteen male Sprague-Dawley rats, 300–400 grams, were housed in an appropriate manner. The middle cerebral artery (MCA) occlusion model was generated as described elsewhere with modifications (26, 27). In short, rats were anesthetized with an intramuscular injection of a mixture of Zoletil (15 mg/kg) and Rompun (10 mg/kg). Rectal temperature, respiration, and heart rate were monitored and maintained in the physiological range throughout the procedure. The right common, internal, and external carotid arteries were exposed through a midline cervical incision. After ligation of the right common and external carotid arteries, a 4-0 nylon monofilament with a tip rounded by gentle heating was introduced via the right internal carotid artery to occlude the proximal MCA, distal internal cerebral artery, and anterior communicating artery. After an hour of transient occlusion of the MCA, the 4-0 nylon monofilament was removed to restore cerebral blood flow. A total of thirteen rats were included in this study.

MRI Acquisition

Animal MR imaging was performed using a 3-T system (Achieva, Philips, Best, the Netherlands) and an 8-channel SENSE wrist coil. Rats were anesthetized with an intramuscular injection of a mixture of Zoletil (15 mg/kg) and Rompun (10 mg/kg).

Dynamic Contrast-Enhanced MRI

MRI acquisition was set at 12 hours, 18 hours, and 36 hours after reperfusion to observe permeability parameters. Rats were imaged 12 hours after reperfusion (n = 3); 18 hours after reperfusion (n = 7); and 36 hours after reperfusion (n = 3). The tail vein was accessed and prepared for the intravenous injection of contrast media before obtaining the MR images. For DCE-MRI, precontrast 3-dimensional T1-weighted images were obtained with the following parameters: field of view (FOV), 60 x 60 mm^2; matrix, 112 x 112; slice thickness, 4.4 mm; slice increment, 2.2 mm; and flip angle of 5°. After the precontrast scan, 60-dynamic contrast-enhanced T1-weighted images were taken with the same MR parameters except the flip angle was altered to 15° after a bolus injection of 0.2 mmol/kg gadolinium (gadobutrol, Gadovist; Bayer, Berlin, Germany) with a temporal resolution of 5 seconds. The total scan time for DCE-MRI was 4 minutes and 30 seconds.

Diffusion-Weighted Image

Diffusion-weighted images were acquired to confirm the acute infarct with the following parameters: FOV, 60 x 60 mm^2; matrix, 128 x 126; slice thickness, 2 mm; and slice gap, 0.2 mm. The diffusion gradient was set at a b-value of 600 s/mm^2.

T2-Weighted Gradient Echo Image*

T2*-weighted gradient echo images were acquired to evaluate hemorrhagic transformations with the following parameters: FOV, 60 x 60 mm^2; matrix, 192 x 192; slice thickness, 2 mm; and slice gap, 0.2 mm.

Evans Blue Injection and Brain Extraction

Evans blue extravasation has been used as a method of evaluating the integrity of BBB (28-30). Evans blue was injected immediately after the last MR acquisition. Using the tail vein, 4 mL/kg of 2% Evans blue (Sigma-Aldrich, St. Louis, MO, USA) in normal saline was injected. A lethal dose of anesthesia was administered 10 hours after the Evans blue injection. The rat brain was transcardially perfused with 4% paraformaldehyde. After brain extraction, the specimen was cooled on ice and then cut into 2-mm coronal sections. The posterior surface of each section was photographed by a digital camera.

Korean Journal of Radiology
KJR

Analysis of MRI

Permeability parameters were calculated by off-line PRIDE tools provided by Philips Medical Systems (Best, The Netherlands), which is based on the pharmacokinetic model of Tofts et al. (31). The two compartment model of Tofts assumes intravascular and extravascular extracellular spaces, which are divided by the BBB. The degree of contrast leakage from the intravascular space to the extravascular extracellular space is referred to as K^{trans}. The volume fraction of the extravascular extracellular space is referred to as v_e. The volume fraction of plasma space is referred to as v_p. Those permeability parameters were calculated by means of iteration between time-intensity curves of the artery and tissue in assumption of the Tofts model (27, 31). Arterial input function was measured at the area of left internal carotid artery (Fig. 1A) and its time-concentration curve was checked (Fig. 1B). Because extravasation of Evans blue was prominent near the slices of Bregma-1.60 mm, they were targeted for analysis. Briefly, post-processing consisted of motion correction of pixels from dynamic images, T1-mapping using different flip angles (5° and 15°), co-registration of pixels on the T1-map, arterial input function estimation, and pharmacokinetic modeling. All these processes were automatically performed by PRIDE tools. Different regions of interest (ROIs) were placed in the cortex and basal ganglia in the ipsilateral and contralateral hemispheres of transient MCA occlusion. Therefore, four different ROIs were drawn per rat. Then, the three types of permeability parameters (K^{trans}, v_e, and v_p) were calculated on each ROI.

Analysis of Specimen

The posterior surface of each section was photographed (Fig. 2A). Photographs of the posterior surface of Bregma-1.60 mm were loaded on Image J (32). The photography of the specimen was split into three color channels: red, green, and blue. Because red-channel images showed good contrast between the normal appearing brain and leakage of Evans blue, red-channel images were used for the analysis of optical density. Mean optical density was measured by ROIs in the ipsilateral cortex (Fig. 2B) and basal ganglia (Fig. 2C) along with contralateral cortex and basal ganglia. Optical density of the corpus callosum was used for normalization of those ROIs. Normalized optical densities were calculated with the following equation: (optical density of corpus callosum - optical density of ROI) / optical density of corpus callosum.

Statistical Analysis

Optical density was taken as the dependent variable and permeability parameters were considered as the independent variables. Scatter plots were drawn between optical densities and permeability parameters of each ROI (n = 52) and fitted linear correlation lines were calculated for each permeability parameter. Pearson correlation analysis was performed. The correlation coefficient and the coefficient of determination were calculated. Durbin-Watson statistic was calculated to assess normality and independence of residuals. For the statistical analysis, we used the statistical software package, SPSS (version 20, SPSS Inc., Chicago, IL, USA). Statistical significance was set at $p < 0.05$.

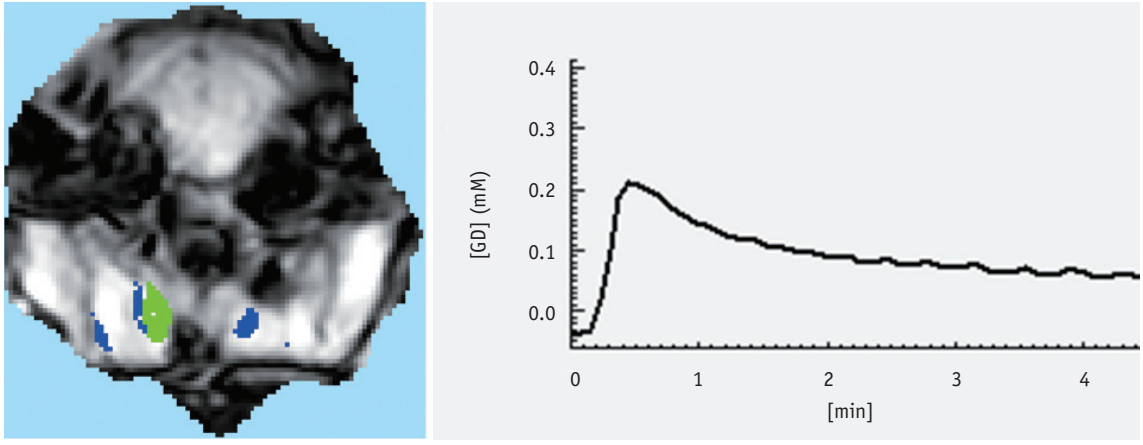

Fig. 1. Selection of arterial input function (AIF) for analysis of permeability parameters.
A. Region of interest was set at region of left cervical internal carotid artery (green color). Venous flow is depicted in blue. **B.** Time-concentration of gadolinium curve showed rapid upslope and early peak of gadolinium concentration (GD), suggestive of appropriate selection of arterial flow.

RESULTS

Thirteen rats showed acute infarct in right basal ganglia or cortex on diffusion-weighted images. There were no cases showing hemorrhagic transformation on T2*-weighted gradient echo images. DCE-MRI showed an increase in permeability parameters in the ipsilateral hemisphere of the MCA occlusion (Fig. 3). There were no cases with a positive value of any permeability parameter in the contralateral normal-appearing hemisphere on DCE-MRI. All the permeability parameters showed a linear correlation with optical density (Table 1, Fig. 4). Among those permeability parameters, K^{trans} showed the highest values of correlation coefficient and coefficient of determination (0.687 and 0.473 respectively, $p < 0.001$). Durbin-Watson statistics for analysis of residuals showed 2.072, which was suggestive of normality and independence of residuals.

DISCUSSION

Dynamic contrast-enhanced MRI is a method of quantification of BBB permeability. In this study, we successfully acquired DCE-MRI in a rat model and analyzed permeability parameters using the pharmacokinetic two compartment model of Tofts. K^{trans} was consistent regarding the prediction of the later extravasation of Evans

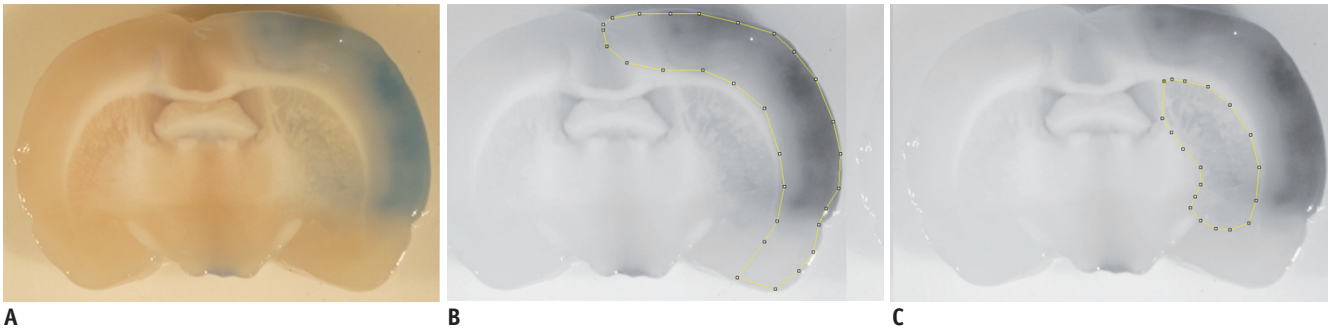

Fig. 2. Analysis of optical density.
A. Posterior surface of sliced specimen (Bregma-1.60) was prepared for analysis of extravasation of Evans blue. ROIs were placed in right cortex **(B)** and basal ganglia **(C)** for measurement of optical density.

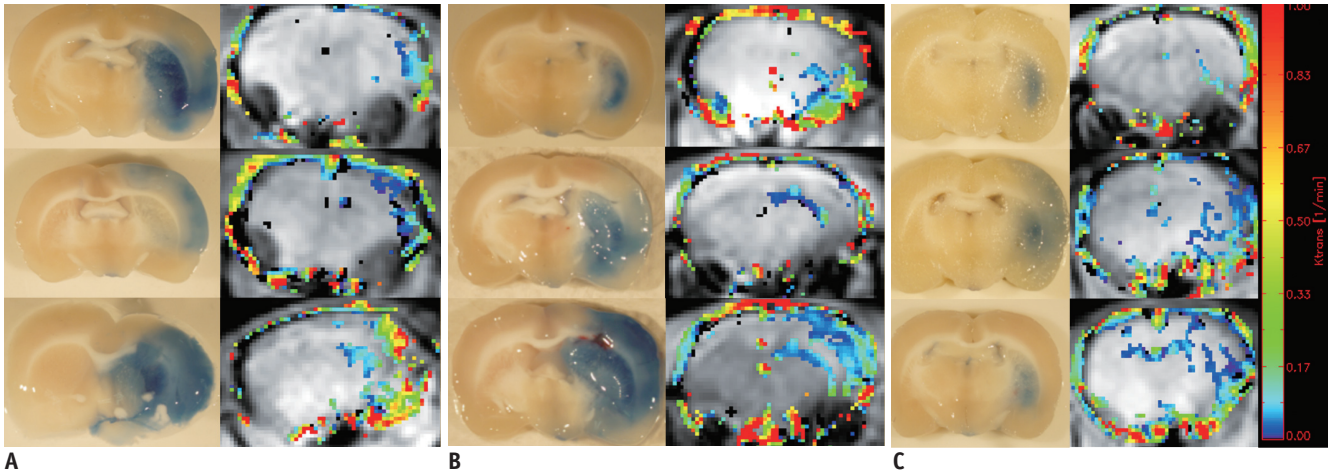

Fig. 3. Extravasation of Evans blue and K^{trans} map.
Extravasation of Evans blue was displayed on left column and K^{trans} map on right column in 12 hours after reperfusion **(A)**, 18 hours after reperfusion **(B)**, and 36 hours after reperfusion **(C)**.

Table 1. Results of Linear Correlation Analysis (n = 52)

	Correlation Coefficient	Coefficient of Determination	Standard Error of Estimate	*P*	Durbin-Watson
K^{trans} (min^{-1})	0.687	0.473	0.145	< 0.001	2.072
v_e	0.471	0.222	0.176	< 0.001	2.379
v_p	0.436	0.190	0.179	0.001	2.429

Korean Journal of Radiology
KJR

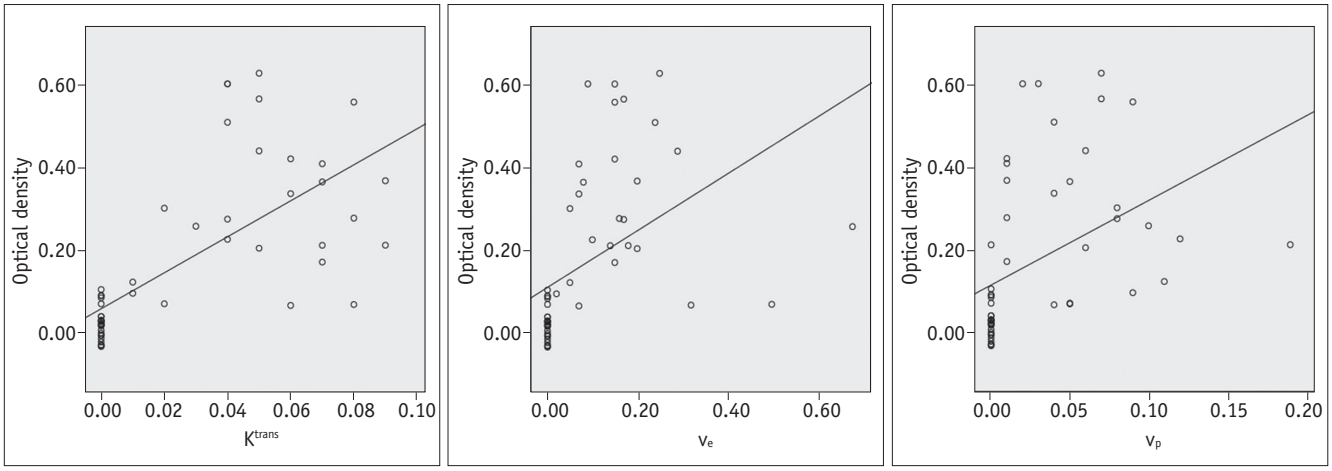

Fig. 4. Scatter plots and fitted linear correlation lines of optical density versus permeability parameters. K^{trans} **(A)**, v_e **(B)**, and v_p **(C)**.

blue in this study. Previous research about permeability mainly focused on K^{trans}, but this study also showed other permeability parameters (v_e and v_p) in terms of their correlation with the extravasation of Evans blue. Previous results in animal models were typically performed using 4.7-T, 7-T, or higher tesla animal-dedicated MR systems and coils (30, 33-37). In this study, we applied 3-T MRI and an 8-channel wrist coil to evaluate permeability in a rat stroke model. Compared with previous studies with higher tesla MRI, our permeability images were inferior in voxel size and temporal resolution. However, all DCE-MRI in our series were interpretable by means of the pharmacokinetic model of Tofts and correlated with later extravasation of Evans blue.

Our data showed that the measured permeability parameters were correlated with a later extravasation of Evans blue. The most correlative parameter among them was K^{trans}. This result is consistent with those of previous studies, even though there was little difference in the methodology of analysis (34, 35). Increased K^{trans} detected 3 hours after embolic infarct has been associated with progression in fibrin leakage (34). Permeability parameters were sensitive to the prediction of later hemorrhage as early as three hours after the embolic infarct and K^{trans} was more sensitive than v_e (35). We thought K^{trans} showed highest correlation with Evans blue leakage because K^{trans} is a targeted quantitative parameter of the BBB between the intravascular and extracellular spaces. However, our results also showed positive correlations between both v_e and v_p and the extravasation of Evans blue. Those two values are related to the concentration of extravasated gadolinium in extracellular and intravascular spaces respectively. Compared with neuro-oncologic DCE-MRI studies, those parameters have been rarely investigated in stroke research. Because our study cannot sufficiently explain about the extracelluar and intravascular spaces in a transient cerebral ischemic model, further research should be performed to examine correlations with cellular integrity (i.e., infarct core and penumbra), cerebral blood volume, and blood flow.

Permeability parameters are quantifiable data which can be candidates for imaging biomarkers in stroke treatment. Compared with histology-based methods, MRI-based methods are better for use in longitudinal studies. MRI enables the repeated scanning of a rat without sacrifice. Serial imaging throughout the entire experiment can eliminate inter-group variance, and therefore offer higher statistical power. Further research using DCE-MRI is necessary to provide information about BBB leakage which is related to post-ischemic edema, hemorrhagic transformation, and neurotoxicity. This can be potentially applied to the clinical management of stroke and the development of neuro-protective agents.

Our study has several limitations. We did not consider the status of reperfusion, which can be evaluated by MR angiography of perfusion-weighted MRI, in our evaluation of the permeability parameters. Status of reperfusion, timing of reperfusion, and status of collaterals might affect the result of permeability changes. In the case of failed reperfusion, the gadolinium bolus may not reach the leaky vessels. This might result in an underestimation of K^{trans}. Secondly, Evans blue extravasation was considered to be a reference standard to assess altered vascular permeability. However, the extent and density of permeability measured by MRI was different because there were innate differences

in tracer characteristics including molecular weight, electric charge, and protein binding between gadolinium and Evans blue. Thirdly, there was a 10-hour interval between the last MR examination time and brain extraction time. The time interval between the Evans blue injection and brain extraction was usually an hour or two in previous studies. However, some of the previous studies used longer time intervals, such as 24 hours (28). In our study, the permeability parameters from DCE-MRI could be predictive of Evans blue extravasation after 10 hours. Finally, we could not evaluate the permeability parameters for the prediction of later hemorrhage, because no case showed a later hemorrhagic transformation. This may be due to an insufficient BBB injury during the MCA occlusion periods or because there was no injection of thrombolytic agents.

In conclusion, permeability parameters (K^{trans}, v_e, and v_p) obtained with DCE-MRI at 3-T are well-correlated with later Evans blue extravasation, which was evaluated in a rat transient cerebral ischemic model, and K^{trans} shows the strongest correlation among the parameters measured.

REFERENCES

1. Tissue plasminogen activator for acute ischemic stroke. The National Institute of Neurological Disorders and Stroke rt-PA Stroke Study Group. *N Engl J Med* 1995;333:1581-1587
2. Lansberg MG, Albers GW, Wijman CA. Symptomatic intracerebral hemorrhage following thrombolytic therapy for acute ischemic stroke: a review of the risk factors. *Cerebrovasc Dis* 2007;24:1-10
3. Tanne D, Kasner SE, Demchuk AM, Koren-Morag N, Hanson S, Grond M, et al. Markers of increased risk of intracerebral hemorrhage after intravenous recombinant tissue plasminogen activator therapy for acute ischemic stroke in clinical practice: the Multicenter rt-PA Stroke Survey. *Circulation* 2002;105:1679-1685
4. Intracerebral hemorrhage after intravenous t-PA therapy for ischemic stroke. The NINDS t-PA Stroke Study Group. *Stroke* 1997;28:2109-2118
5. Barber PA, Demchuk AM, Zhang J, Buchan AM. Validity and reliability of a quantitative computed tomography score in predicting outcome of hyperacute stroke before thrombolytic therapy. ASPECTS Study Group. Alberta Stroke Programme Early CT Score. *Lancet* 2000;355:1670-1674
6. Kase CS, Furlan AJ, Wechsler LR, Higashida RT, Rowley HA, Hart RG, et al. Cerebral hemorrhage after intra-arterial thrombolysis for ischemic stroke: the PROACT II trial. *Neurology* 2001;57:1603-1610
7. Larrue V, von Kummer RR, Müller A, Bluhmki E. Risk factors for severe hemorrhagic transformation in ischemic stroke patients treated with recombinant tissue plasminogen activator: a secondary analysis of the European-Australasian Acute Stroke Study (ECASS II). *Stroke* 2001;32:438-441
8. Lansberg MG, Thijs VN, Bammer R, Kemp S, Wijman CA, Marks MP, et al. Risk factors of symptomatic intracerebral hemorrhage after tPA therapy for acute stroke. *Stroke* 2007;38:2275-2278
9. Alsop DC, Makovetskaya E, Kumar S, Selim M, Schlaug G. Markedly reduced apparent blood volume on bolus contrast magnetic resonance imaging as a predictor of hemorrhage after thrombolytic therapy for acute ischemic stroke. *Stroke* 2005;36:746-750
10. Kim EY, Na DG, Kim SS, Lee KH, Ryoo JW, Kim HK. Prediction of hemorrhagic transformation in acute ischemic stroke: role of diffusion-weighted imaging and early parenchymal enhancement. *AJNR Am J Neuroradiol* 2005;26:1050-1055
11. Hacke W, Albers G, Al-Rawi Y, Bogousslavsky J, Davalos A, Eliasziw M, et al. The Desmoteplase in Acute Ischemic Stroke Trial (DIAS): a phase II MRI-based 9-hour window acute stroke thrombolysis trial with intravenous desmoteplase. *Stroke* 2005;36:66-73
12. Olivot JM, Mlynash M, Thijs VN, Kemp S, Lansberg MG, Wechsler L, et al. Relationships between infarct growth, clinical outcome, and early recanalization in diffusion and perfusion imaging for understanding stroke evolution (DEFUSE). *Stroke* 2008;39:2257-2263
13. Bang OY, Saver JL, Alger JR, Shah SH, Buck BH, Starkman S, et al. Patterns and predictors of blood-brain barrier permeability derangements in acute ischemic stroke. *Stroke* 2009;40:454-461
14. Selim M, Fink JN, Kumar S, Caplan LR, Horkan C, Chen Y, et al. Predictors of hemorrhagic transformation after intravenous recombinant tissue plasminogen activator: prognostic value of the initial apparent diffusion coefficient and diffusion-weighted lesion volume. *Stroke* 2002;33:2047-2052
15. Lin K, Kazmi KS, Law M, Babb J, Peccerelli N, Pramanik BK. Measuring elevated microvascular permeability and predicting hemorrhagic transformation in acute ischemic stroke using first-pass dynamic perfusion CT imaging. *AJNR Am J Neuroradiol* 2007;28:1292-1298
16. Hom J, Dankbaar JW, Soares BP, Schneider T, Cheng SC, Bredno J, et al. Blood-brain barrier permeability assessed by perfusion CT predicts symptomatic hemorrhagic transformation and malignant edema in acute ischemic stroke. *AJNR Am J Neuroradiol* 2011;32:41-48
17. Lin K. Predicting transformation to type 2 parenchymal hematoma in acute ischemic stroke by CT permeability imaging. *AJNR Am J Neuroradiol* 2011;32:E124; author reply E125
18. Kassner A, Roberts T, Taylor K, Silver F, Mikulis D. Prediction of hemorrhage in acute ischemic stroke using permeability MR imaging. *AJNR Am J Neuroradiol* 2005;26:2213-2217
19. Kassner A, Roberts TP, Moran B, Silver FL, Mikulis DJ. Recombinant tissue plasminogen activator increases blood-brain barrier disruption in acute ischemic stroke: an MR imaging permeability study. *AJNR Am J Neuroradiol*

2009;30:1864-1869
20. Larsson HB, Courivaud F, Rostrup E, Hansen AE. Measurement of brain perfusion, blood volume, and blood-brain barrier permeability, using dynamic contrast-enhanced T(1)-weighted MRI at 3 tesla. *Magn Reson Med* 2009;62:1270-1281
21. Thornhill RE, Chen S, Rammo W, Mikulis DJ, Kassner A. Contrast-enhanced MR imaging in acute ischemic stroke: T2* measures of blood-brain barrier permeability and their relationship to T1 estimates and hemorrhagic transformation. *AJNR Am J Neuroradiol* 2010;31:1015-1022
22. Warach S, Latour LL. Evidence of reperfusion injury, exacerbated by thrombolytic therapy, in human focal brain ischemia using a novel imaging marker of early blood-brain barrier disruption. *Stroke* 2004;35(11 Suppl 1):2659-2661
23. Sandoval KE, Witt KA. Blood-brain barrier tight junction permeability and ischemic stroke. *Neurobiol Dis* 2008;32:200-219
24. Wang CX, Shuaib A. Critical role of microvasculature basal lamina in ischemic brain injury. *Prog Neurobiol* 2007;83:140-148
25. Dirnagl U, Iadecola C, Moskowitz MA. Pathobiology of ischaemic stroke: an integrated view. *Trends Neurosci* 1999;22:391-397
26. Ahn SK, Hong S, Park YM, Lee WT, Park KA, Lee JE. Effects of agmatine on hypoxic microglia and activity of nitric oxide synthase. *Brain Res* 2011;1373:48-54
27. Kassner A, Mandell DM, Mikulis DJ. Measuring permeability in acute ischemic stroke. *Neuroimaging Clin N Am* 2011;21:315-325, x-xi
28. Kamada H, Yu F, Nito C, Chan PH. Influence of hyperglycemia on oxidative stress and matrix metalloproteinase-9 activation after focal cerebral ischemia/reperfusion in rats: relation to blood-brain barrier dysfunction. *Stroke* 2007;38:1044-1049
29. Belayev L, Busto R, Ikeda M, Rubin LL, Kajiwara A, Morgan L, et al. Protection against blood-brain barrier disruption in focal cerebral ischemia by the type IV phosphodiesterase inhibitor BBB022: a quantitative study. *Brain Res* 1998;787:277-285
30. Strbian D, Durukan A, Pitkonen M, Marinkovic I, Tatlisumak E, Pedrono E, et al. The blood-brain barrier is continuously open for several weeks following transient focal cerebral ischemia. *Neuroscience* 2008;153:175-181
31. Tofts PS, Brix G, Buckley DL, Evelhoch JL, Henderson E, Knopp MV, et al. Estimating kinetic parameters from dynamic contrast-enhanced T(1)-weighted MRI of a diffusable tracer: standardized quantities and symbols. *J Magn Reson Imaging* 1999;10:223-232
32. Schneider CA, Rasband WS, Eliceiri KW. NIH Image to ImageJ: 25 years of image analysis. *Nat Methods* 2012;9:671-675
33. Durukan A, Marinkovic I, Strbian D, Pitkonen M, Pedrono E, Soinne L, et al. Post-ischemic blood-brain barrier leakage in rats: one-week follow-up by MRI. *Brain Res* 2009;1280:158-165
34. Jiang Q, Ewing JR, Ding GL, Zhang L, Zhang ZG, Li L, et al. Quantitative evaluation of BBB permeability after embolic stroke in rat using MRI. *J Cereb Blood Flow Metab* 2005;25:583-592
35. Ding G, Jiang Q, Li L, Zhang L, Gang Zhang Z, Ledbetter KA, et al. Detection of BBB disruption and hemorrhage by Gd-DTPA enhanced MRI after embolic stroke in rat. *Brain Res* 2006;1114:195-203
36. Taheri S, Candelario-Jalil E, Estrada EY, Rosenberg GA. Spatiotemporal correlations between blood-brain barrier permeability and apparent diffusion coefficient in a rat model of ischemic stroke. *PLoS One* 2009;4:e6597
37. Neumann-Haefelin C, Brinker G, Uhlenküken U, Pillekamp F, Hossmann KA, Hoehn M. Prediction of hemorrhagic transformation after thrombolytic therapy of clot embolism: an MRI investigation in rat brain. *Stroke* 2002;33:1392-1398